

## DEVELOPING NANOSTRUCTURED COMPOSITE OF TITANIUM DIOXIDE AND POLY(TRIAZINE IMIDE) FOR SELECTIVE PHOTOOXIDATION

**M.S. Golovin, A.T. Mironova, V.P. Zakharchenkova, S.A. Sozykin, O.I. Bol'shakov**  
South Ural State University, Chelyabinsk, Russia  
✉ golovinms@susu.ru

**Abstract.** Pristine semiconductors are rarely suggested as efficient heterogenous photocatalysts, as they exhibit low efficiency, due to high recombination rate and narrow adsorption spectrum. Instead, various composites are proposed where intimate contact between two phases creates heterojunction, that improves photoactivity. In this report, we disclose a stepwise development of a grain-based hierarchical structure of photoactive composite based on anatase and poly(triazine imide) (PTI). This nanocomposite was efficient in benzyl alcohol (BA) oxidation and provided targeted benzaldehyde (BAI) with 94 % selectivity at 100 % conversion.

**Keywords:** poly(triazine imide), titanium dioxide, photocatalysis

**Acknowledgments.** This work was funded by Ministry of Science and Higher Education of the Russian Federation (agreement № 075-15-2022-1135) and South Ural State University.

**For citation:** Golovin M.S., Mironova A.T., Zakharchenkova V.P., Sozykin S.A., Bol'shakov O.I. Developing nanostructured composite of titanium dioxide and poly(triazine imide) for selective photooxidation. *Bulletin of the South Ural State University. Ser. Chem.* 2024;16(4):184–190. DOI: 10.14529/chem240418

Научная статья  
УДК 544.478-03  
DOI: 10.14529/chem240418

## РАЗРАБОТКА НАНОСТРУКТУРИРОВАННОГО КОМПОЗИТА НА ОСНОВЕ ДИОКСИДА ТИТАНА И ПОЛИ(ТРИАЗИН ИМИДА) ДЛЯ СЕЛЕКТИВНОГО ФОТООКИСЛЕНИЯ

**М.С. Головин, А.Т. Миронова, В.П. Захарченкова, С.А. Созыкин, О.И. Большаков**  
Южно-Уральский государственный университет, г. Челябинск, Россия  
✉ golovinms@susu.ru

**Аннотация.** Немодифицированные полупроводники редко применяются в качестве гетерогенных фотокатализаторов, поскольку они демонстрируют низкую эффективность из-за высокой скорости рекомбинации и узкого спектра поглощения света. Вместо этого предлагаются различные композиты, в которых тесный контакт между двумя фазами создает гетеропереход, улучшающий фотоактивность. В этом отчете мы описываем разработку фотоактивного композита на основе анатаза и поли(триазинимида) (ПТИ), который показал 100 % конверсию и 94 % селективность бензальдегида (БА).

**Ключевые слова:** поли(триазин имид), диоксид титана, фотокатализ

**Благодарности.** Эта работа финансировалась Министерством науки и высшего образования РФ (соглашение № 075-15-2022-1135) и Южно-Уральским государственным университетом.

**Для цитирования:** Developing nanostructured composite of titanium dioxide and poly(triazine imide) for selective photooxidation / M.S. Golovin, A.T. Mironova, V.P. Zakharchenkova et al. // Вестник ЮУрГУ. Серия «Химия». 2024. Т. 16, № 4. С. 184–190. DOI: 10.14529/chem240418

**Introduction.** Selective oxidation of alcohols to aldehydes is one of the most important reactions in the industrial synthesis of organic compounds. Such processes, as a rule, are quite complex to implement

and are harmful to the nature as it consumes hazardous reagents. For this reason, it is necessary to search for new, greener ways to synthesize these substances [1]. Benzaldehyde is an indispensable component in the production of a wide range of medicines, perfumes, dyes, and food flavors. The industrial production of this aldehyde is based on the selective catalytic oxidation of toluene. The reaction is quite simple, but its disadvantages are harsh reaction conditions and consumption of additional reagents [2–4]. Photoactivated chemical processes seem as a reasonable response to a growing demand for environmentally benign chemical technologies [5]. The advantages of photocatalysis over classical synthesis are mild conditions: room temperature, atmospheric pressure, reagentlessness.

Poly(triazine imide) (PTI) is a highly crystalline polymorph of carbon nitride. It is an affordable, inexpensive semiconductor, which is resistant to photocorrosion [6]. Its structure contains basic Lewis and Brønsted centers, which increase its activity in various catalytic processes [7]. The photocatalytic use of PTI is mainly limited to laboratory due to the disadvantage of rapid charge recombination. The optimal way to increase the photoactivity of carbon nitride is to produce composite photocatalysts with another semiconductor. This way, higher efficiency is achieved by improved charge separation, preventing charge recombination [8] and widened adsorption spectrum [9].

Titanium dioxide is one of the most promising materials for the formation of photoactive composites with PTI with type 2 heterojunction [10]. Optimal promising method of composite formation is hydrothermal treatment. It allows to ensure intimate contact of 2 phases [11, 12]. In this work, a series of TiO<sub>2</sub>@PTI composites were prepared and showed excellent results in photo oxidation of BA.

### Experimental part

**Equipment.** JEOL JSM 7001F, Rigaku Ultima IV diffractometer, Netzsch 449 F1, Shimadzu IRAffinity-1S FTIR sp., Shimadzu UV-2700 UV-vis sp., HPLC Shimadzu Prominence LC-20.

**Synthesis of TiO<sub>2</sub>@PTI composite.** Ti-peroxo complex was prepared to be the precursor of the TiO<sub>2</sub> phase. For this, 5 mL of aqueous ammonia (NH<sub>3(aq)</sub>, 30%) was added to the 15 mL solution containing 0.4 g of titanium oxysulfate (TiOSO<sub>4</sub>). The resulting colloidal titanium dioxide (TiO<sub>2</sub>) was then centrifuged, washed with deionized water 8 times and redissolved with 4 mL of Hydrogen peroxide (H<sub>2</sub>O<sub>2</sub>, 30%). The pH of the solution was adjusted to (3, 5, 7 or 9) with aqueous ammonia (NH<sub>3(aq)</sub>, 30%), and the volume was filled up to 20 mL with distilled water. Then, this solution was put into a 40 mL autoclave with the PTFE lining containing a different amount of PTI powder (50, 100, 200 or 400 mg). The autoclave was heated at a specified temperature and treatment time. After cooling, the obtained solid was washed 3 times and dried at 100 °C.

**Photocatalytic reaction.** The photocatalytic performance of was studied in the oxidation of benzyl alcohol (BA) to benzaldehyde (BAI) in acetonitrile on air. Benzyl alcohol solution in acetonitrile (30 ml, 2 mM) together with 50 mg of photocatalyst were placed into a water jacketed quartz reactor. The quartz reactor was irradiated with thirty 1 Wt UV-diodes with a sharp luminosity peak at 395 nm, a light power of 600 W/m<sup>2</sup> and constant stirring on a magnetic stirrer; the irradiation time was 5 hours, on air at 20 °C. Samples were filtered through a PTFE syringe filter prior to HPLC analysis. An HPLC calibration curve was established using BA and BAI with concentrations: 2, 1.5, 1, 0.5, 0.2, and 0.1 mM.

### Results and discussion

**Photocatalytic studies.** In search of the optimal composite photocatalyst, we adapted hydrothermal synthesis employing Ti-peroxo complex as a precursor of TiO<sub>2</sub> mixed with prefabricated PTI. Various parameters of hydrothermal synthesis was considered for screening, which were all optimized step by step. Efficiency criterion was the yield of the benzaldehyde in a standard single-stage reaction of photocatalytic oxidation of BA involving synthesized composites as photocatalysts. Also, before each experiment, the photocatalyst and reaction mixture were stirred for half an hour in the dark to establish adsorption equilibrium. No significant change was detected in the concentration of reagents in the mixture. Table 1 shows the results of photocatalytic tests of samples with different optimization parameters. To begin with, a previously developed method of composite formation was used, in which the Ti-peroxo complex equilibrated at pH 9 was hydrothermally treated with 200 mg of PTI for 3 days [13]. Firstly, the effect of hydrothermal treatment time on the photocatalytic properties of the samples was studied. Sample after 3 days of treatment showed the best result. Next, we studied the effect of the starting Ti-peroxo complex pH on the photocatalyst functional properties. We did not try a higher pH of the media, as it

dissolves the PTI [14]. The next optimization parameter was the temperature of the hydrothermal synthesis. A set of obtained samples showed that the lower the temperature provided the most efficient photocatalyst. Photocatalytic tests were also carried out with a batch of samples which were synthesized with various amounts of PTI at fixed amount of Ti-peroxo complex. An increase in the starting PTI content in the starting mixtures leads to an improvement in photocatalytic characteristics.

Table 1

Optimization of hydrothermal synthesis of TiO<sub>2</sub>@PTI composite

Entry	Condition parameters	BA conversion, %	Selectivity to BAI, %	BAI yield, %	Other products, %	Pseudo 1 <sup>st</sup> order cons., h <sup>-1</sup>	AQE, %
Effect of hydrothermal treatment time							
1	1 day	49.8	99.6	49.6	0.2	0.138	0.170
2	3 days	<b>56.4</b>	<b>99.9</b>	<b>56.4</b>	<b>0</b>	<b>0.166</b>	<b>0.197</b>
3	5 days	48.4	93.8	45.4	3	0.132	0.150
Effect of pH of Ti-peroxo complex							
4	pH3	33.3	99.5	33.1	0.2	0.081	0.124
5	pH5	30.4	98.9	30.1	0.3	0.072	0.112
6	pH7	39.0	99.0	38.6	0.2	0.042	0.070
7	pH9	<b>56.4</b>	<b>99.9</b>	<b>56.4</b>	<b>0</b>	<b>0.166</b>	<b>0.197</b>
Effect of synthesis temperature							
8	100 °C	<b>56.4</b>	<b>99.9</b>	<b>56.4</b>	<b>0</b>	<b>0.166</b>	<b>0.197</b>
9	140 °C	9.0	19.8	1.8	7.2	0.019	0.007
10	180 °C	23.6	49.1	11.6	12	0.054	0.040
Effect of the amount of added PTI during synthesis							
11	50 mg	32.8	87.3	28.7	4.1	0.080	0.112
12	100 mg	29.6	95.5	28.3	1.3	0.070	0.103
13	200 mg	56.4	99.9	56.4	0	0.166	0.197
14	400 mg	<b>71.9</b>	<b>99.5</b>	<b>71.5</b>	<b>0.4</b>	<b>0.253</b>	<b>0.267</b>
Comparison of the composite with pristine phase samples							
15	TiO <sub>2</sub>	38.1	99.9	38.1	0	0.096	0.145
16	PTI	76.8	87.3	67.0	9.8	0.270	0.251

**Physicochemical characteristics of TiO<sub>2</sub>@PTI composite.** Figures 1a,b depict microphotographs where photocatalyst is represented by nanostructured titanium dioxide grains that envelop the surface of poly(triazine imide) aggregates. Nanograins are 200–300 nm in length and 60–80 nm in width.

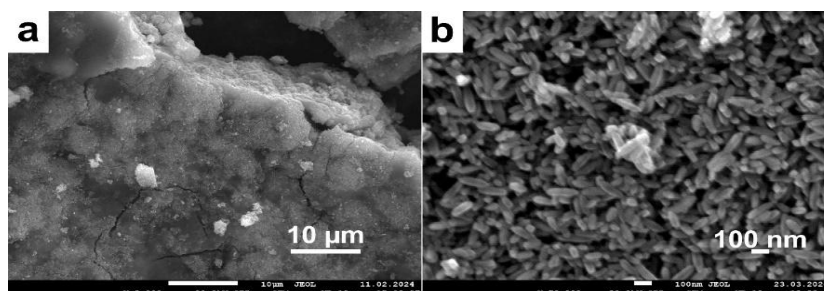


Fig. 1. SEM images of composite TiO<sub>2</sub>@PTI sample (a) x2000 (a) x50000

X-ray diffraction (Fig. 2a) was used to characterize the TiO<sub>2</sub>@PTI sample. The composite's pXRD profile exhibits reflexes of two phases. Anatase phase (JCPDS Card no. 21-1272) is manifested by reflexes at 25.2°, 37.7°, 47.9°, 53.8°, 54.9° 2θ degrees [15,16]. Poly(triazine imide) phase is represented by a series of peaks at 12.0°, 20.9° and 32.1° 2θ degrees [17], respectively. TiO<sub>2</sub>@PTI shows a significant change in the reflex positions, such that the most intense one at 26.5° is shifted by 0.9° toward larger angles compared to pristine phase. It shows partial incorporation of titanium dioxide particles into the PTI matrix, changing of distance between layers and the formation of a composite [18].

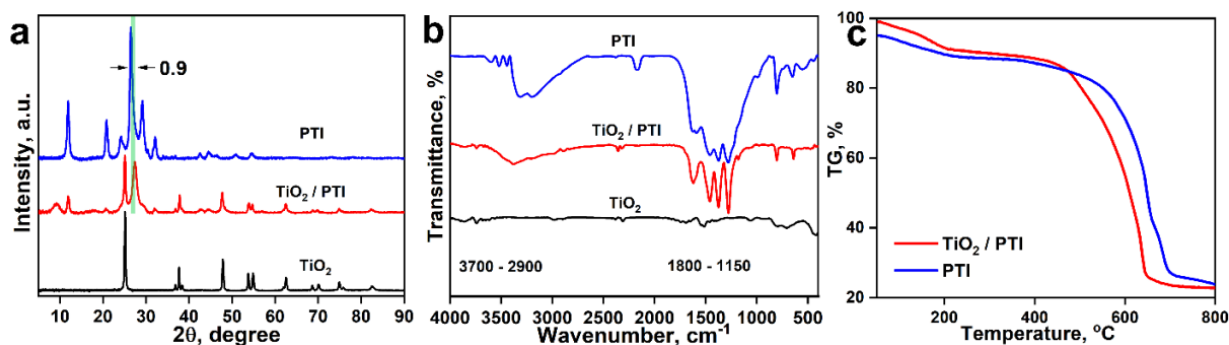


Fig. 2 (a) XRD patterns; (b) FTIR spectra of samples; (c) Comparison TG curves of samples

IR spectra of the samples are shown in Fig. 2b. Spectra of  $\text{TiO}_2$  demonstrate broad bands near  $3700\text{--}3400\text{ cm}^{-1}$ ,  $1800\text{--}1450\text{ cm}^{-1}$ , related to the vibrations of OH groups and  $400\text{--}900\text{ cm}^{-1}$ , corresponding to vibrations of the Ti–O–Ti lattice [19]. The composite's absorption bands related to  $\text{TiO}_2$  are not visible because of their low intensity compared to the vibrations of the organic fragments of PTI. Absorption bands of poly(triazine imide) and composites in the “fingerprint region” up to  $1800\text{ cm}^{-1}$  exhibit same profile. The peak at  $808\text{ cm}^{-1}$  is the “breathing mode” of triazine units, bands at  $1800\text{--}1150\text{ cm}^{-1}$  correspond to the stretching vibrations of s-triazine units [20]. The differences in the spectra of  $\text{TiO}_2\text{@PTI}$  and pristine PTI is the absence of a peak at  $2170\text{ cm}^{-1}$  related to vibrations of cyano groups, as well as a narrowed set of bands at  $1800\text{--}1150\text{ cm}^{-1}$ . Their hydrolysis of cyano fragment at alkaline conditions could be one of the explanation.

Thermal analysis of the  $\text{TiO}_2\text{@PTI}$  are shown in Fig. 2c. Three main stages can be distinguished on the TG curves. The first stage (up to  $200\text{ }^\circ\text{C}$ ) is physisorbed water desorption. The second stage is a partial oxidation of organic substances (up to  $600\text{ }^\circ\text{C}$ ). Third stage is combustion of PTI (higher  $600\text{ }^\circ\text{C}$ ). The significant difference in the combustion temperature of the PTI phase resembles the low-temperature shift in the decomposition of the  $g\text{-C}_3\text{N}_4$  phase in its composites [21]. With this thermal behavior of the synthesized sample, we assume the composite is formed by close contact between phases.

UV spectroscopy studies of the samples (Fig. 3 a,b) revealed the several adsorption maxima composites in the composite material, which indicates the presence of several band gaps [22, 23]. The optical band gap was calculated from the linear approximation of the largest straight segment of the spectrum after the Kubelka-Munk transformation [24]. The calculated main band gap of the composite was found to be  $2.11\text{ eV}$ , which was a significant drop, compared to pristine PTI ( $2.85\text{ eV}$ ) and  $\text{TiO}_2$  ( $3.25\text{ eV}$ ).

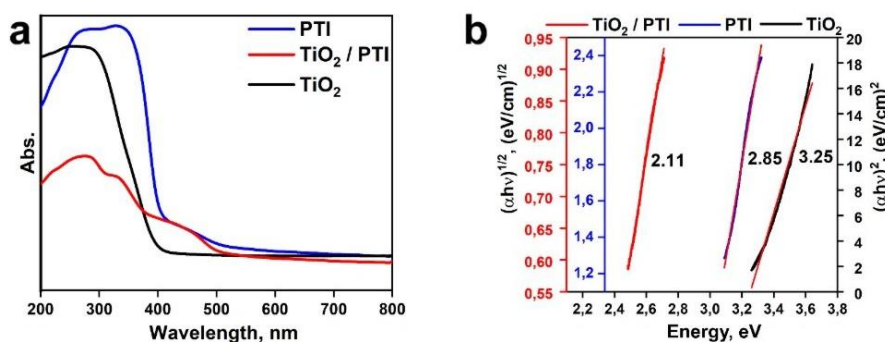


Fig. 3 (a) UV-vis spectra of PTI,  $\text{TiO}_2\text{@PTI}$ ,  $\text{TiO}_2$ ; (b) Optical band gap of samples

**Practical applicability** of the optimal  $\text{TiO}_2\text{@PTI}$  photocatalyst was examined at prolonged irradiation. The complete conversion was achieved after 10 hours of irradiation, providing with a good selectivity of 94% Fig. 4a. The reaction is described by a pseudo-first-order kinetic model, as shown in Fig. 4b, in agreement with previous reports about heterogeneous photocatalysts. Figure 4c shows a comparison of chromatograms of commercial BA and the reaction mixture after photocatalysis (at 9.8 min) using a  $\text{TiO}_2\text{@PTI}$  composite. The chromatogram of the reaction mixture shows benzoic acid (8.1 min), but the peak area is insignificant.

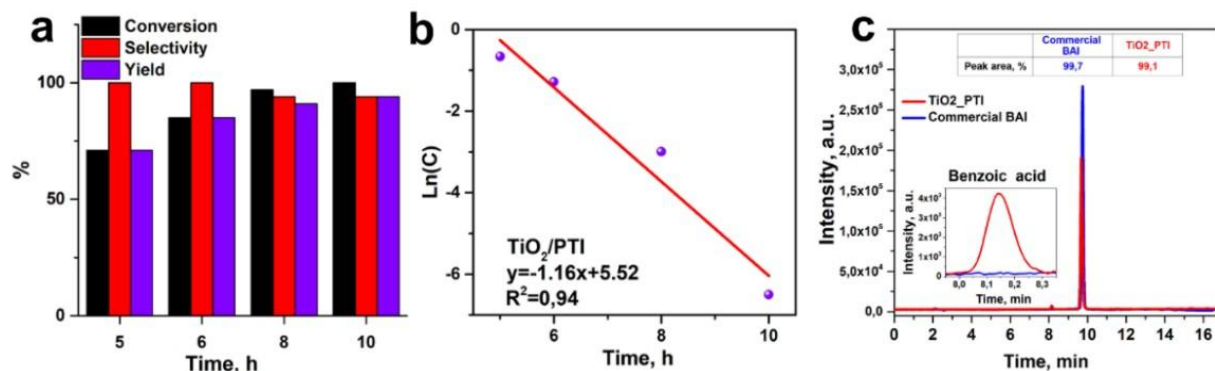


Fig. 4. (a) Kinetics of BA photooxidation using  $\text{TiO}_2\text{@PTI}$ ; (b) linear fit of the quasi-first-order kinetic model; (c) HPLC chromatograms of commercial BAI and reaction mixture using  $\text{TiO}_2\text{@PTI}$  sample

Scavenger test (Table 2) revealed that p-Benzoquinone diminished selectivity. It speaks for active  $\text{O}_2\cdot$  radical involvement in the selective oxidation. Application of methanol alcohol used to “trap”  $\text{OH}\cdot$  radicals showed a decrease in conversion by 2 times, showing their major role in the reaction [25]. Based on obtained data, we hypothesize that the reaction follows a complex mechanism: exposure of the  $\text{TiO}_2\text{@PTI}$  material with light causes the formation of a pair of photoseparated charges (an electron, a “hole”). An electron, interacting with  $\text{O}_2$ , forms a superoxide radical. “Hole” reacts with BA, forms a BA radical. Further, the resulting superoxide radical and BA radical react to form BAI [25]. Reaction with sun light showed 24,1% conversion.

Table 2

Influence of scavengers and solar irradiation on photocatalytic oxidation of benzyl alcohol

Entry	Scavenger	BA conver., %	Selectivity to BAI, %	BAI yield, %	Other products, %	Pseudo 1 <sup>st</sup> order cons., h <sup>-1</sup>	AQE, %
	$\text{TiO}_2\text{@PTI}$ (pure)	71.9	99.5	71.5	0.4	0.253	0.267
1	p-Benzoquinone	61.9	80.9	50.0	11.9	0.193	0.186
2	MeOH	32.0	99.9	32.0	0	0.077	0.120

## Conclusions

For the first time, a composite nanomaterial based on titanium dioxide and poly(triazine imide) was used for the photocatalytic synthesis of BA. Photocatalytic properties were optimized by screening hydrothermal conditions, providing material with improved selectivity. Major factor influencing photoactivity of the resulting composite was the starting ratio of components and the temperature of the synthesis. The photocatalyst comprised discrete 200–300 nm long and 60–80 nm wide grains. Strong interaction between phases was confirmed with pXRD, thermal analysis and UV-spectroscopy, creating a heterojunction for widened adsorption spectrum. The photocatalyst showed the highest value of conversion (100%) and selectivity (94%).

## References

1. Belousov A.S., Suleimanov E.V. // G. Ch. The R. S. of Ch., 2021. V. 23, No 17. P. 6172. DOI: 10.1039/D1GC01690C.
2. Fazlı H., Akkol Ç., Osmanoğulları S. et al. // J. Organomet. Chem. Elsevier, 2023. V. 983. P. 122553. DOI: 10.1016/j.jorganchem.2022.122553.
3. Song H., Liu Z., Wang Y. et al. // Green Energy Environ., 2019. V. 4, No 3. P. 278. DOI: 10.1016/J.GEE.2018.09.001.
4. Bao X., Lv X., Wang Z. et al. // Int. J. Hyd. En. P., 2021. V. 46, No 76. P. 37782. DOI: 10.1016/j.ijhydene.2021.09.052.
5. Pomilla F., García-López E., Marci G. et al. // M. T. Sustain., 2021. V. 13. P. 100071. DOI: 10.1016/j.mtsust.2021.100071.
6. Morozov R., Golovin M., Uchaev D. et al. // JCSS., 2021. V. 133, No 133. P. 1. DOI: 10.1007/S12039-021-01999.

7. Thomas A., Fischer A., Goettmann F. et al. // J. Mater. Chem. The Royal S. of Chem., 2008. V. 18, No. 41. P. 4893–4908. DOI: 10.1039/B800274F.
8. Tay Q., Wang X., Zhao X. et al. // Journal of Catalysis, 2016. V. 342. P. 55. DOI: 10.1016/j.jcat.2016.07.007.
9. Marschall R. // Adv. F. Mat. John Wiley & Sons, Ltd, 2014. V. 24, No 17. P. 2421. DOI: 10.1002/ADFM.201303214.
10. Baca M., Kukulka W., Cendrowski K. et al. // C.SusChem.2019. V. 12, No 3. P. 612. DOI: 10.1002/cssc.201801642.
11. Yan H., Yang H. // J. Alloys Compd. Elsevier, 2011. V. 509, No 4. P. L26. DOI: 10.1016/j.jallcom.2010.09.201.
12. Zárate R., Fuentes S., Wiff J. et al. // J. Phys. Ch. Solids. 2007. V. 68, No 4. P. 628. DOI: 10.1016/j.jpcs.2007.02.011.
13. El-Akaad S., Morozov R., Golovin M. et al. // Talanta. 2022. V. 238. P. 123025. DOI: 10.1016/j.talanta.2021.123025.
14. Horvath-Bordon E., Kroke E., Svoboda I. et al. // DT. The RS. Ch., 2004. No 22. P. 3900. DOI: 10.1039/B412517G.
15. Theivasanthi T., Alagar M. // Chemical Physics, 2013. arXiv:1307.1091 <https://arxiv.org/abs/1307.1091v1>.
16. Wei X, Zhu G, Fang J. et al. // Int. J. P. J. Wiley & Sons, Ltd, 2013. V. 2013, No 1. P. 726872. DOI: 10.1155/2013/726872.
17. Ham Y., Maeda K., Cha D. // Chem. – An Asian J. J. W. & Sons, Ltd, 2013. V. 8, No 1. P. 218. DOI: 10.1002/ASIA.201200781.
18. Yan X., Ning G., Zhao P. // MDPI., 2019. V. 9, No 1. P. 55. DOI:10.3390/CATAL9010055.
19. Zhang B., Wang Q., Zhuang J. et al. // J. Photochem. Photobiol. A Chem. 2018. V. 362. P. 1. DOI: <https://doi.org/10.1016/j.jphotochem.2018.05.009>.
20. Zhu Z., Pan H., Gong J. et al. // Appl. Catal. B Env., Elsevier, 2018. V. 232. P. 19. DOI: 10.1016/j.apcatb.2018.03.035.
21. Tseng I., Sung Y., Chang P. et al. // Polymers (Basel). 2019. V. 11, No 1. P. 1. DOI: 10.3390/polym11010146.
22. Li J., Liu Y., Li H. et al. // JPP. A Chem., 2016. V. 317. P. 151. DOI: 10.1016/J.JPHOTOCHEM.2015.11.008.
23. Wang C., Zhu W., Xu Y. et al. // Ceram. Int. 2014. V. 40, No 8. P. 11627. DOI: 10.1016/J.CERAMINT.2014.03.156
24. Valencia S., Marín J.M., Restrepo G. // TOM. Sc. J., 2010. V. 4, No 2. P. 9. DOI: 10.2174/1874088X01004020009.
25. Zhao L., Zhang B., Xiao X. et al. // J. M. C. A Ch., 2016. V. 420. P. 82. DOI: 10.1016/J.MOLCATA.2016.03.012.

**Mikhail S. Golovin** – research associate of Nanotechnology Research and Education Centre, South Ural State University, Chelyabinsk, Russia. E-mail: golovinms@susu.ru

**Anastasiya T. Mironova** – laboratory researcher, Research & Innovation Services, South Ural State University, Chelyabinsk, Russia. E-mail: mironovaat@susu.ru

**Valeriya P. Zakharchenkova** – student of Department of Ecology and Chemical Technology, South Ural State University, Chelyabinsk, Russia. E-mail: lerazakhar@gmail.com

**Sergey A. Sozykin** – Ph.D. (Physical and Mathematical Sciences), docent, Department of Physics of Nanoscale Systems, South Ural State University, Chelyabinsk, Russia. E-mail: sozykinsa@susu.ru

**Oleg I. Bol'shakov** – Ph.D. (Chemistry), senior researcher of Nanotechnology Research and Education Centre, South Ural State University, Chelyabinsk, Russia. E-mail: bolshakovoi@susu.ru

**Головин Михаил Сергеевич** – научный сотрудник НОЦ «Нанотехнологии», Южно-Уральский государственный университет, Челябинск, Россия. E-mail: golovinms@susu.ru

**Миронова Анастасия Тарасовна** – лаборант-исследователь УНИД, Южно-Уральский государственный университет, Челябинск, Россия. E-mail: mironovaat@susu.ru

**Захарченкова Валерия Петровна** – студент, кафедра «Экология и химическая технология», Южно-Уральский государственный университет, Челябинск, Россия. E-mail: lerazakhar@gmail.com

**Созыкин Сергей Анатольевич** – кандидат физико-математических наук, доцент кафедры «Физика наноразмерных систем», Южно-Уральский государственный университет, Челябинск, Россия. E-mail: sozykinsa@susu.ru

**Большаков Олег Игоревич** – кандидат химических наук, старший научный сотрудник НОЦ «Нанотехнологии», Южно-Уральский государственный университет, Челябинск, Россия. E-mail: bolshakovoi@susu.ru

*The article was submitted 22 August 2024.*

*Статья поступила в редакцию 22 августа 2024 г.*